JMEPEG (2005) 14:747-754
DOI: 10.1361/105994905X75556

1059-9495/$19.00

Phase-Stability Dependence of Plastic Deformation Behavior in Ti-Nb-Ta-Zr-O Alloys

J. Hwang, S. Kuramoto, T. Furuta, K. Nishino, and T. Saito

(Submitted August 24, 2005)

The authors investigated the effects of alloy content on mechanical properties to make clear a correlation between plastic deformation behavior and β-phase stability in Ti-Nb-Ta-Zr-O alloys. It was realized that there was specific compositional area in which the alloy exhibited little work hardening and minimum Young's modulus value. The specific area was expressed by the bond order (Bo), based on the *DV-X*α method, of 2.87 and the averaged electron/atom ratio (e/a) of 4.24, which corresponded to those of a multifunctional β titanium alloy, "Gum Metal." These electronic conditions also minimized ideal strength required for plastic deformation without any dislocation activity. The deformation behavior of alloys in the specific compositional area revealed that the unique behavior could be characterized by a "giant fault." It was also confirmed that such a compositional area corresponded to the phase boundary between the α″ martensite and β phases at room temperature.

Keywords β-phase stability, plastic deformation behavior, work hardening, Young's modulus

1. Introduction

The newly developed titanium alloy, "Gum Metal", is a multifunctional alloy (Ref 1, 2), which when compared with general metallic materials has an ultra-low elastic modulus with high strength (Fig. 1), large-elastic deformation (2.5%) (Fig. 2a), superplastic nature permitting cold plastic working to 99.9% or more with no work hardening at room temperature, an ultra-high strength of more than 2000 MPa by applying a heat treatment (Fig. 2b), a near-zero linear expansion coefficient (Invar property, Fig. 2c), and a constant elastic modulus (Elinvar property) over a wide temperature range from −200 to +250 °C (Fig. 2d). Gum Metal is presently used for eyeglass frames and precision screws because these characteristics are suitable for such applications. All of these unique characteristics are achieved by cold working. We have already reported that the unique characteristics of Gum Metal are attributable to a peculiar feature in its plastic deformation behavior, which is accompanied by numerous "giant faults" formed without the aid of dislocation glide (Ref 3). In a cold-worked alloy, this plastic deformation mechanism forms elastic strain fields of hierarchical structures ranging in size from nanometers to several tens of micrometers.

Gum Metal is a β titanium alloy having a body-centered cubic (bcc) structure. This alloy is fundamentally expressed as Ti_3(Ta + Nb + V) + (Zr, Hf) + O and has three electronic magic numbers: (a) an average valence electron number of approximately 4.24; (b) a "bond order" (Bo) of about 2.87 based on the *DV-X*α cluster method (Ref 4), which represents its bonding strength; and (c) a *d* electron-orbital energy level (*Md*) of about 2.45 eV, representing electronegativity. The parameters of e/a, *Md*, and Bo values are indices that relate to β-phase stability and depend on alloy composition. Therefore, these three "magic numbers" mean that the characteristics of Gum Metal correlate strongly with β-phase stability. Hence, it is important to know how the properties and plastic deformation behavior are affected by alloy composition. In this paper, the authors investigate the mechanical properties and plastic deformation behavior of Ti-Nb-Ta-Zr-O alloys to clarify the effect of β-phase stability on the peculiar characteristics of Gum Metal.

2. Experimental Procedure

The β-phase stability was controlled by changing the niobium content in alloys having the typical Gum Metal compo-

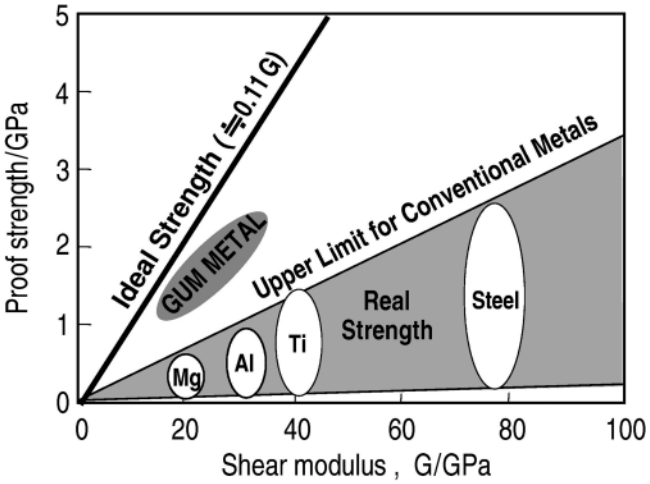

Fig. 1 Relationship between strength and shear modulus

This paper was presented at the Beta Titanium Alloys of the 00's Symposium sponsored by the Titanium Committee of TMS, held during the 2005 TMS Annual Meeting & Exhibition, February 13-16, 2005 in San Francisco, CA.

J. Hwang, S. Kuramoto, T. Furuta, K. Nishino, and **T. Saito,** Toyota Central R&D Laboratories Inc., 41-1, Yokomichi, Nagakute, Aichi, 480-1192, Japan. Contact e-mail: hwang@mosk.tytlabs.co.jp.

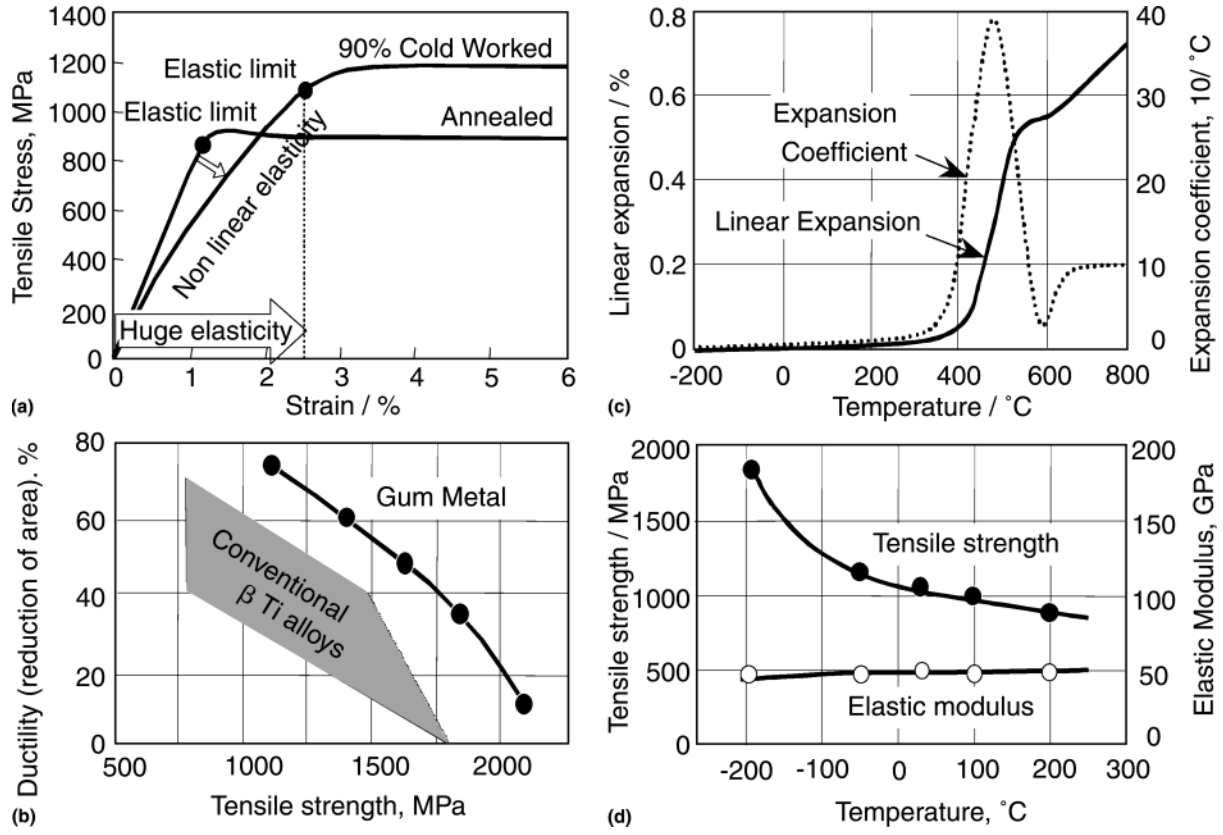

Fig. 2 Typical properties of Gum Metal: (a) stress-strain curve, (b) relationship between strength and ductility, (c) Invar property, and (d) Elinvar property

Table 1 Compositions of experimental alloys

	Comp.	Nb	Ta	Zr	e/a	Bo	*Md*		Comp.	Nb	Ta	Zr	e/a	Bo	*Md*
Binary alloys	20-0-0	2	0	0	4.20	2.85	2.44	Ternary alloys	20-0-2	20	0	2	4.20	2.86	2.45
	21-0-0	2	0	0	4.21	2.85	2.44		21-0-2	21	0	2	4.21	2.86	2.45
	22-0-0	2	0	0	4.23	2.86	2.44		23-0-2	23	0	2	4.23	2.87	2.45
	23-0-0	2	0	0	4.23	2.86	2.44		24-0-2	24	0	2	4.24	2.87	2.45
	24-0-0	2	0	0	4.24	2.86	2.44		25-0-2	25	0	2	4.25	2.87	2.45
	26-0-0	2	0	0	4.26	2.87	2.44		26-0-2	26	0	2	4.26	2.88	2.45
	27-0-0	2	0	0	4.27	2.87	2.44		20-0.7-0	20	0.7	0	4.21	2.85	2.44
	34-0-0	3	0	0	4.34	2.90	2.44		21-0.7-0	21	0.7	0	4.22	2.86	2.44
Quarternary alloys	16-0.7-2	1	0	2	4.17	2.85	2.45		23-0.7-0	23	0.7	0	4.24	2.86	2.44
	20-0.7-2	2	0	2	4.21	2.86	2.45		24-0.7-0	24	0.7	0	4.25	2.87	2.44
	22-0.7-2	2	0	2	4.23	2.87	2.45		25-0.7-0	25	0.7	0	4.26	2.87	2.44
	23-0.7-2	2	0	2	4.24	2.87	2.45		26-0.7-0	26	0.7	0	4.27	2.87	2.44
	25-0.7-2	2	0	2	4.26	2.88	2.45								
	27-0.7-2	2	0	2	4.27	2.88	2.45								

mol%, Ti; balance, O: 1.2 mol%

sition of Ti-23%Nb-0.7%Ta-2%Zr-1.2%O ("%" here stands for "mol%"). Experimental samples and their calculated values of e/a, Bo, and *Md* are shown in Table 1. Niobium contents are changed between 16 and 34% in binary alloys of Ti-*X*%Nb, ternary alloys of Ti-*X*%Nb-2%Zr and Ti-*X*%Nb-0.7%Ta, and quaternary alloys of Ti-*X*%Nb-0.7%Ta-2%Zr. The mechanical properties and plastic deformation behavior were studied in these alloys to clarify the effect of β-phase stability. The oxygen content of all experimental samples was 1.2%. Although oxygen content is considered to affect β-phase stability, its contribution is not considered for e/a, Bo, and *Md* in Table 1.

Samples were made by the powder metallurgy method. Pure titanium and other powders of the alloying elements were blended, compacted by cold isostatic pressing, and sintered in a vacuum. The sintered compacts were hot-forged, solution-treated, and water-quenched before cold working, which was performed with rotary swaging at room temperature by a reduction in area of 90%. The oxygen content of each sample was determined as 1.14-1.30% with a Horiba EMGA650 oxygen/nitrogen analyzer (Horiba Co., Kyoto, Japan).

Tensile tests were carried out on smooth cylindrical specimens of 2 mm diameter of 10 mm gauge length at a strain rate

of 5×10^{-4} s^{-1}. Tensile strain was measured by a strain gauge to precisely determine Young's modulus. Hardness was examined by the Vickers hardness test at a load of 10 kgf, and the value of the work hardening ratio (WHR) was calculated as a ratio of hardness after cold working to that after solution treatment.

Characterization of the microstructure after deformation was conducted by optical microscopy and electron backscattering pattern (EBSP) measurement. Samples for EBSP measurement were prepared by electrolytic polishing of the cross-sectional surface of the cold worked bars in 10% methanol solution of perchloric acid. EBSP was performed on an FEI XL-30S-FEG (FEI Co., OR) with an orientation imaging microscopy (OIM) 3.0 (TexSEM Lab., UT). Moreover, we observed the surface relief generated by indentations of the Vickers hardness tester to characterize plastic deformation behavior. Schematic illustration for this method is shown in Fig. 3.

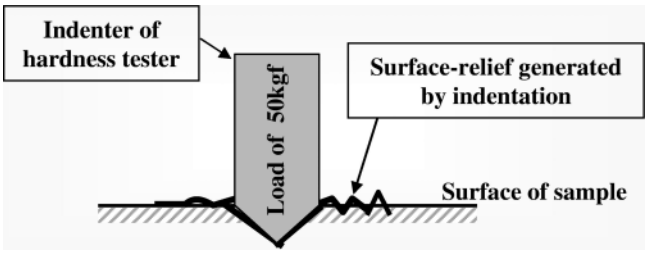

Fig. 3 Schematic illustration for characterization of plastic deformation

3. Results

3.1 Correlation of Tensile Properties and β-Phase Stability

Figure 4 shows the tensile properties of quenched alloys plotted as a relation with Bo, a parameter that shows β-phase stability. Figure 4(b) shows Bo dependence of Young's modulus for all quenched alloys. It is obvious that these Young's modulus correlated well with Bo, and shows their minimum at Bo value around 2.87. Furthermore, Fig. 4(c) shows that elongation could be also arranged by Bo; elongation in each alloy system decreases suddenly at Bo values of 2.86-2.87. Hanada et al. (Ref 5) reported that the plastic deformation mode changed from twin deformations + dislocation glide to dislocation glide at a composition where elongation suddenly decreases in Ti-Nb and Ti-Mo β binary alloys. Therefore, the results in the current study suggest there is a possibility of an abrupt change in plastic deformation mode at Bo values of 2.86-2.87.

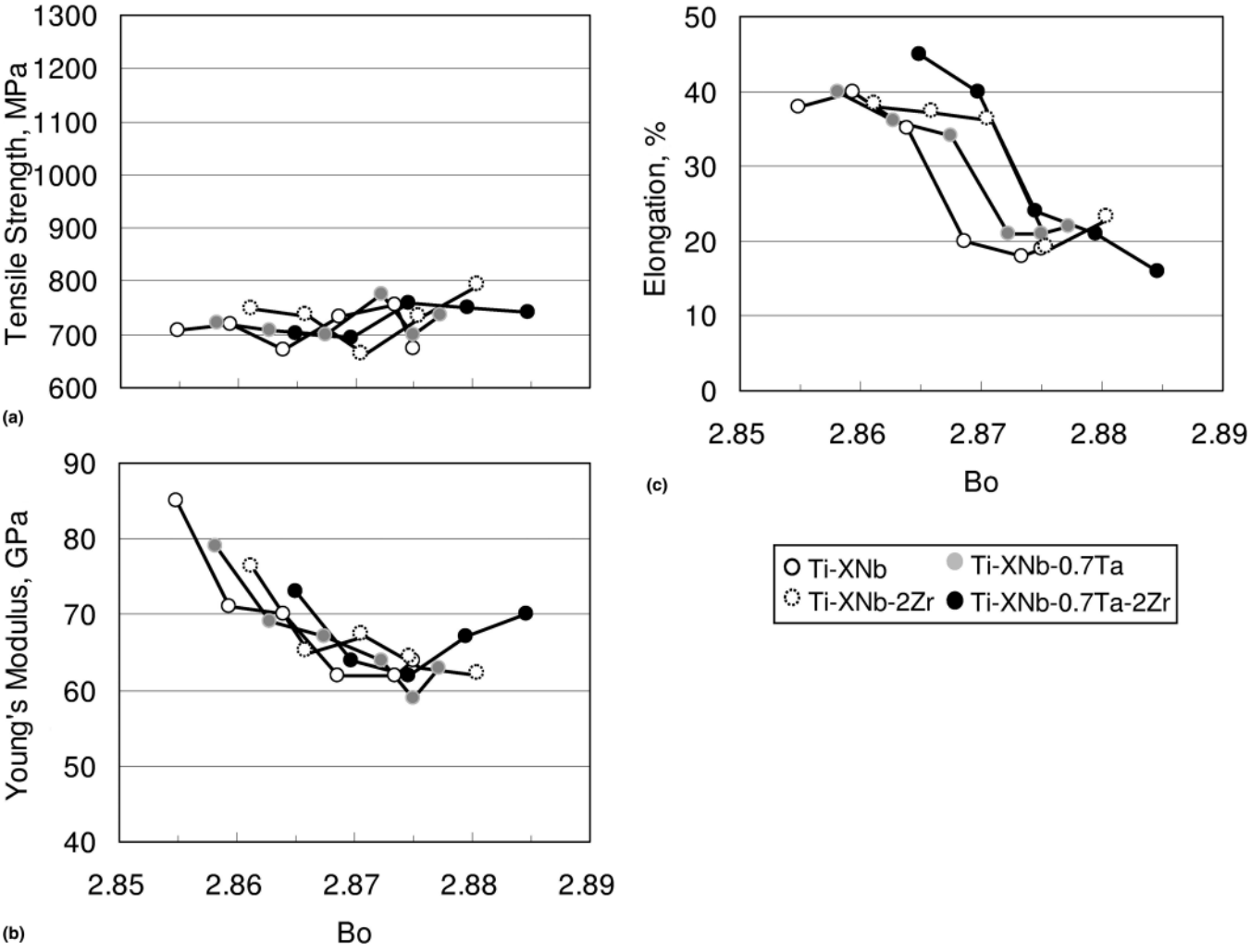

Fig. 4 Relationship between tensile properties and Bo in quenched alloys: (a) tensile strength, (b) Young's modulus, and (c) elongation

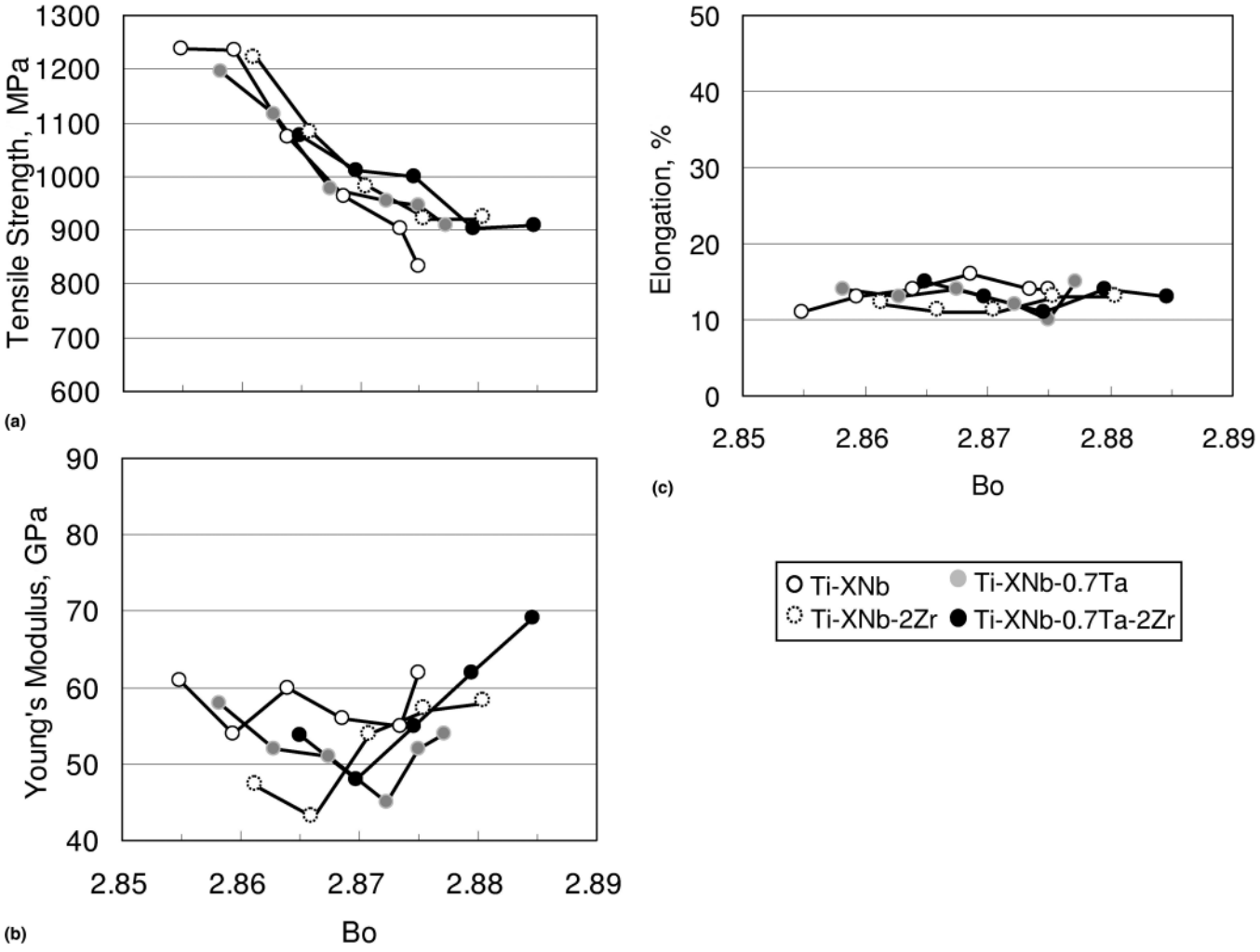

Fig. 5 Relationship between tensile properties and Bo after cold working: (a) tensile strength, (b) Young's modulus, and (c) elongation

This unique characteristic of Gum Metal is obtained by cold working as noted above. Figure 5 shows the tensile properties of cold-worked alloys; tensile strength of all alloys increased by cold working with the increase being larger when Bo was smaller than 2.87. This tendency correlated with the change in the plastic deformation mode noted above. On the other hand, Young's modulus decreases by cold working; the amount is remarkable in alloys that have a lower Bo. Young's modulus of cold-worked alloys is minimized at Bo of 2.86-2.87, although they do not correlate as well with Bo values as do those of quenched materials.

3.2 Correlation of Plastic Deformation Behavior and β-Phase Stability

As noted above, tensile properties of quenched and cold worked materials were revealed to have certain correlations with β-phase stability. Next, the authors describe the relationship between plastic deformation behavior and β-phase stability. First, the authors examined work hardening behavior by calculating the work hardening ratio (WHR), which is the rate of change of hardness between quenched and cold-worked materials for each alloy. Figure 6 shows the change tendency of the WHR by Bo. In all binary, ternary, and quaternary alloys, WHR is well correlated with Bo. WHR is >30% at the lowest

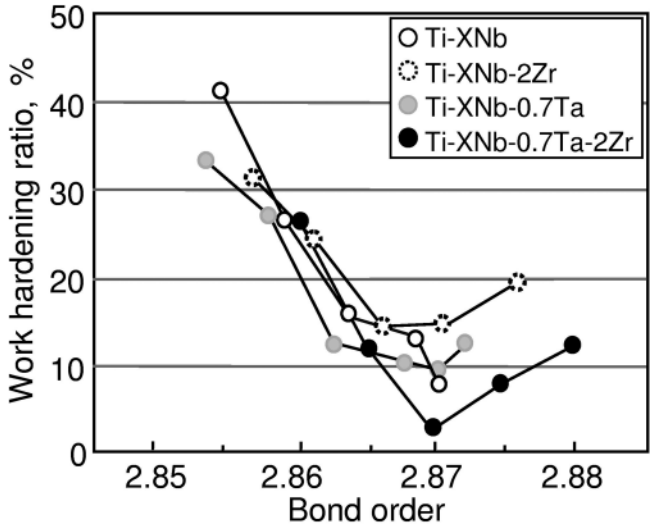

Fig. 6 Relationship between work hardening ratio and Bo

Bo and decreases with increasing Bo. At Bo of 2.87, WHR starts to increase with increasing Bo, that is, the minimum value of WHR is attained in alloys that have Bo of 2.87. The minimum value of WHR in quaternary alloy is as low as 4%,

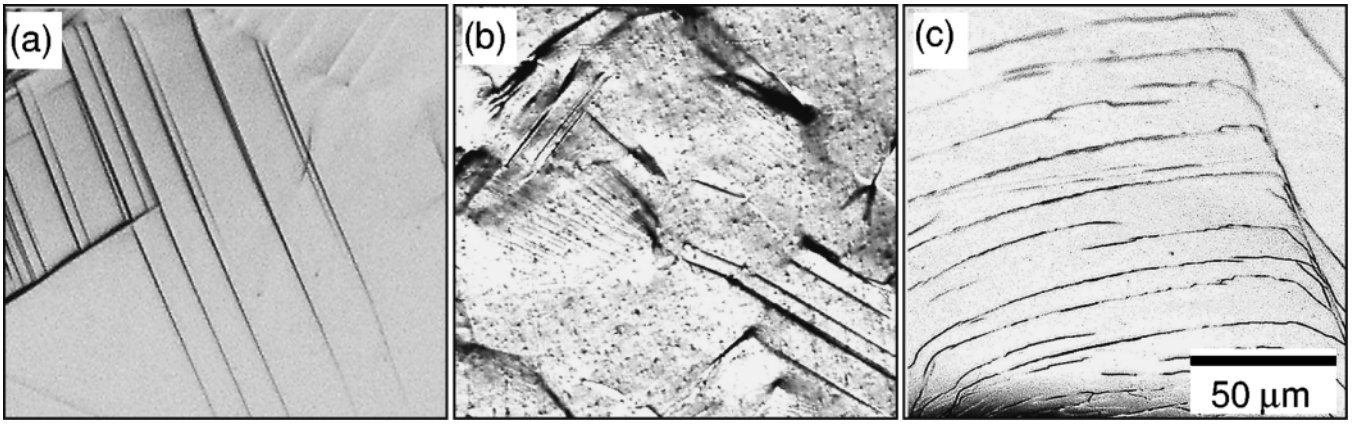

Fig. 7 Typical patterns of surface-relief generated by indentation of hardness tester: (a) 20-0.7-2, (b) 23-0.7-2, and (c) 27-0.7-2

which means that this alloy is hard to work-harden even after severe cold working with reduction in area of 90%.

It is interesting that the WHR is strongly dependent on β-phase stability. The authors next sought to examine the relationship between plastic deformation behavior and β-phase stability, because work hardening is considered to have a close relation to plastic deformation. To characterize plastic deformation behavior, observations were performed of surface relief generated by indentation of the hardness tester. Surface-relief patterns can be roughly divided into three types: Fig. 7(a) shows typical plastic deformation behavior in which the pattern is characterized with straight lines as a result of stress-induced martensite transformation; Fig. 7(c) shows typical plastic deformation behavior characterized with numbers of curved lines brought about by a "pencil glide" dislocation motion frequently observed in bcc metals; Fig. 7(b) shows a type corresponding to the plastic deformation behavior of Gum Metal: the straight lines caused by the compressive load have directionality but are more discontinuous than the other two illustrated deformation behaviors. In addition, some of the steps along the straight lines are deeper than those in the stress-induced martensitic transformation (Fig. 7a). These straight lines are believed to be caused by a unique plastic deformation mechanism (Ref 3).

Figure 8 shows the relationship between plastic deformation behavior and Bo and e/a in all experimental alloys. Stress-induced martensitic transformation is generated in alloys with low Bo and e/a, while dislocation glide is preferable in alloys with high Bo and e/a. On the other hand, alloys around Bo of 2.87 and e/a of 4.24 demonstrate peculiar plastic deformation behavior (Fig. 7b). To examine plastic deformation behavior at a further stage of deformation, microstructures after rotary swaging were observed in three kinds of quaternary alloys: 20-0.7-2, 23-0.7-2, and 27-0.7-2. The microstructures in bar specimens cold worked with a reduction in area of 40% are shown in Fig. 9. Values of Bo and e/a in each alloy are indicated in the figure caption. Lines or bands in grains caused by plastic deformation were observed in Fig. 9(a) and (b), while etch pits are seen as black spots. These lines and bands are considered to correspond to the surface reliefs seen in Fig. 7. Because slip lines were not etched by the etching condition used in the current study, no trace of dislocation glide can be seen in Fig. 9(c). Phase analyses were performed by x-ray diffraction (XRD) to confirm β-phase stability in quenched and cold-worked materials. Some XRD profiles are shown elsewhere (Ref 2). In alloys with Bo lower than 2.87, athermal

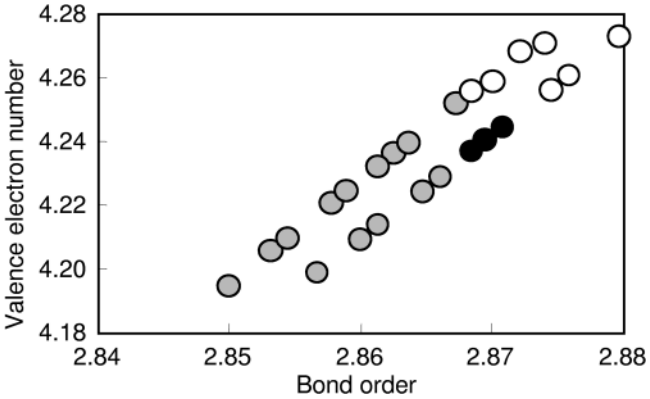

Fig. 8 Relationship between plastic deformation behavior, Bo, and e/a: stress-induced martensitic transformation (gray circles), peculiar plastic deformation (closed circles), and dislocation glide (open circles)

martensite α″ by quenching and stress-induced martensite α″ by cold working were generated. However, alloys that have Bo of 2.87 or higher show β single phase, even after cold working (Ref 2); the composition area around Bo of 2.87 is the phase boundary between α″+β phases and β single phase. XRD studies also confirmed there was no ω phase in the specimens.

4. Discussion

Alloys with Bo of 2.87 and e/a of 4.24 have β single phase and show peculiar plastic deformation behavior. EBSP analyses were carried out to obtain crystallographic information in cold-worked alloys; Fig. 10 shows an example of an EBSP analysis in a bar specimen cold worked by 40% reduction in area for 23-0.7-2 as seen in Fig. 9(b). Crystallographic boundaries over 15° are drawn as solid lines. The initial grain size before cold working is about 100 μm, so many grains can be seen to be divided into several parts by these boundaries. Figure 11 shows point-to-point misorientation along the arrow in Fig. 10. Crossing the boundaries makes crystallographic misorientation at <30°. Twin deformations have been reported to form during plastic deformation in some β titanium alloys. Hanada et al. (Ref 6) reported {112}<111> and {332}<113> twin deformations, in which the rotation angles between the

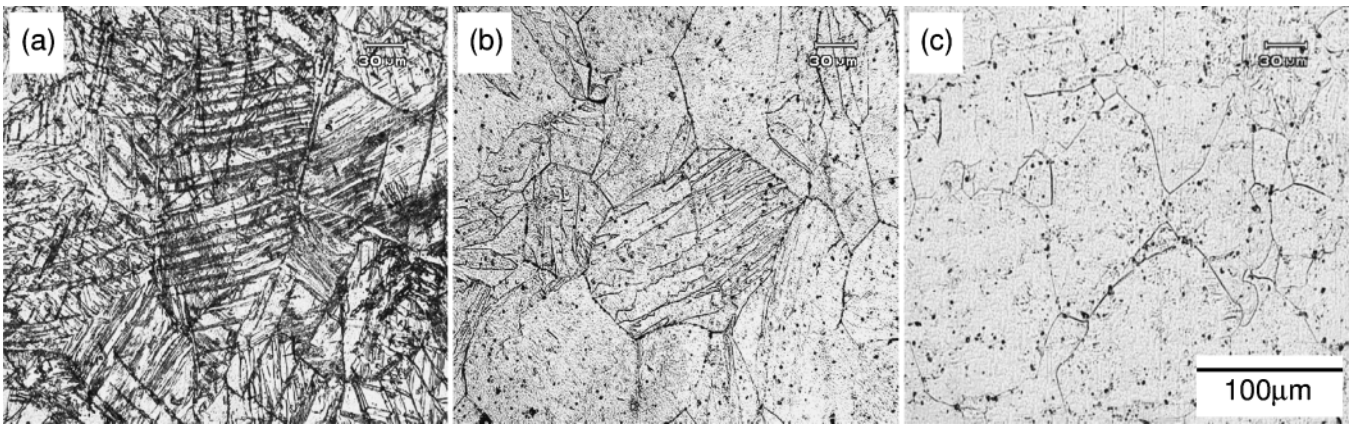

Fig. 9 Microstructures after 40% rotary swaging at room temperature: (a) 20-0.7-2 (Bo, 2.86; e/a, 4.21); (b) 23-0.7-2 (Bo, 2.87; e/a, 4.24); and (c) 27-0.7-2 (Bo, 2.88; e/a, 4.27)

Fig. 10 Boundary map in a bar specimen after 40% rotary swaging at room temperature

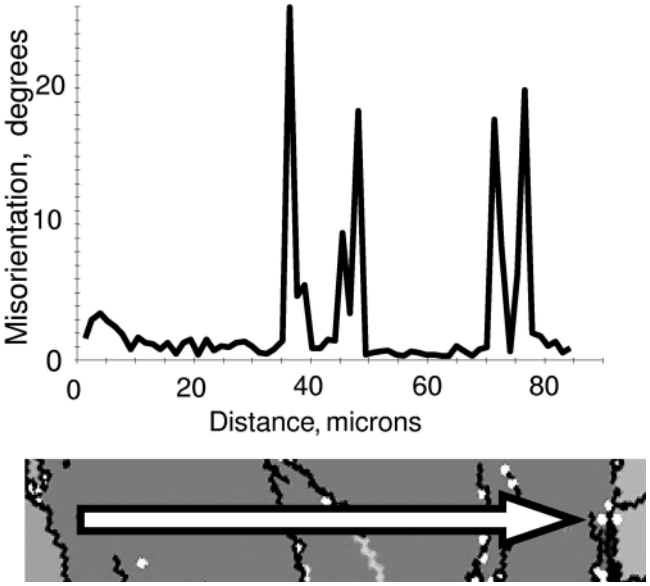

Fig. 11 Point-to-point misorientation plots in Fig. 10

matrix and the twin are 70.3° or 50.3° around the <110> axis in β Ti-Nb and Ti-V binary alloys, respectively. In addition, the authors observed an area of localized distortion along "giant faults" in the quaternary alloy with Bo of 2.87 and e/a of 4.24, in which the crystal rotation is misoriented by 20-30° to the neighboring area (Ref 3). Therefore, the origin of the boundaries shown in Figs. 7 and 9 is different from the conventional twin boundaries. Results of EBSP analyses in the bar specimens cold worked by 80-90% were almost the same as those in specimen cold worked by 40%, excluding deformation texture developed with an increasing amount of cold working.

Figure 12 summarizes Young's modulus and the WHR versus Bo and e/a in the current study. It is obvious that Young's modulus and the WHR depend on Bo and e/a and their values are a minimum in compositions with Bo and e/a in the vicinity of 2.87 and 4.24, respectively. That these alloys with Bo of 2.87 and e/a of 4.24 show peculiar deformation behavior without the aid of dislocation glide, and have the lowest Young's modulus and WHR values at the same time, is most interesting. A discussion followed of the meaning of "Bo of 2.87 and e/a of 4.24" in relation to elastic properties.

First, the authors consider why Young's modulus has a minimum value at Bo of 2.87 and e/a of 4.24. When the elastic constants of the binary β titanium alloys, c_{11}, c_{12}, and c_{14}, are calculated by first-principles calculations (Ref 7), $(c_{11} - c_{12})$ has a strong correlation to e/a and approaches zero at e/a = 4.24. This means that Young's modulus has its smallest value when e/a equals about 4.24. However, from the present results, Young's modulus increases when Bo moves from 2.87 even at e/a of 4.24. Therefore, it is concluded that Young's modulus reaches a minimum value only when two conditions (e/a = 4.24 and Bo = 2.87) are satisfied at the same time in ternary or quaternary alloys.

Next, consider why peculiar plastic deformation behavior, like that in Gum Metal, occurs at Bo of 2.87 and e/a of 4.24. It has been reported that the ideal shear strength of bcc metal is shown by Eq 1 (Ref 3, 8). As stated above, $(c_{11} - c_{12})$ ap-

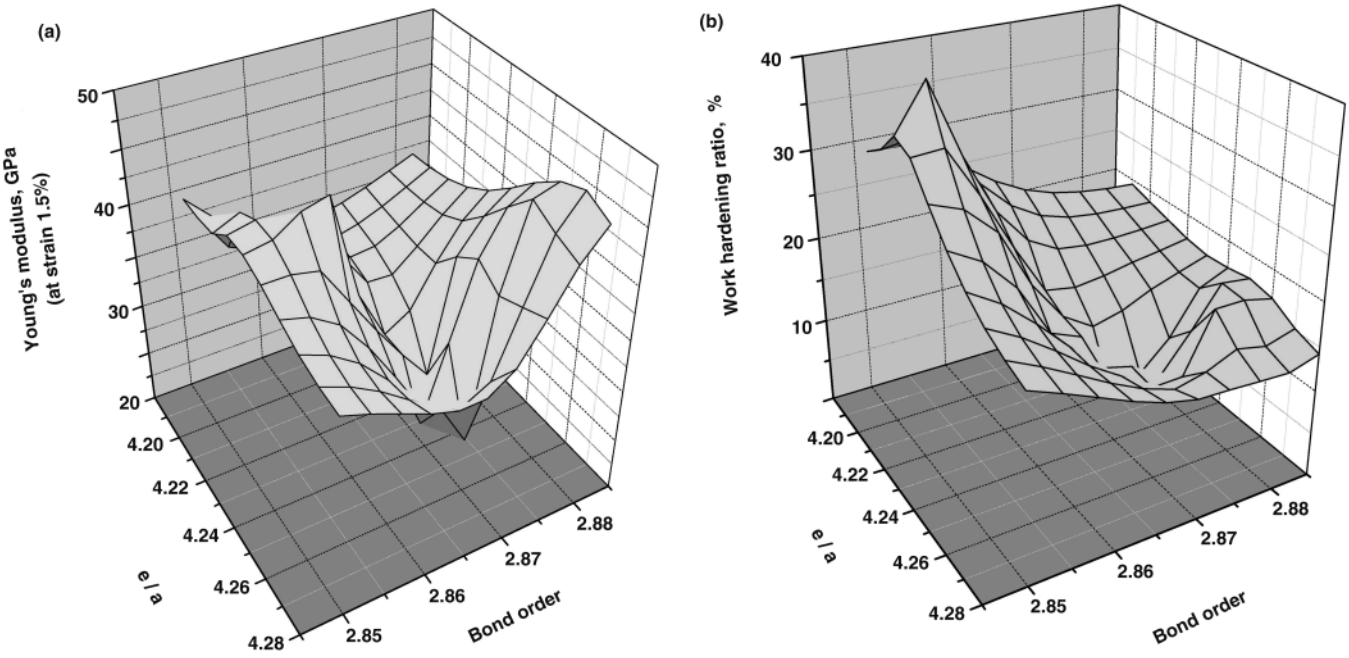

Fig. 12 Dependence of Young's modulus and work hardening ratio on Bo and e/a: (a) Young's modulus and (b) work hardening ratio (WHR)

proaches zero when e/a = 4.24, so the ideal shear strength is expected to reach a very small value.

$$\tau \doteqdot 0.11\, G_{111} = 0.11 \times \frac{3c_{44}(c_{11} - c_{12})}{c_{11} - c_{12} + 4c_{44}} \quad \text{(Eq 1)}$$

The calculated ideal shear strength of Gum Metal was about 1 GPa (Ref 3), a calculated value that is almost equal to the actual tensile strength of Gum Metal of 0.9-1 GPa, as seen in Fig. 1 and 2(a). The ideal strength for pure metals is several dozen times the actual one. The strength can be increased to some extent, such as by alloying, cold working, or heat treatment, but conventional metallic materials are known to have lower strengths than their ideal ones. This gap between ideal and actual strength has been successfully explained by the dislocation theory; however, the ideal strength for Gum Metal is estimated to be so small as to be comparable to its actual strength. The low ideal strength of Gum Metal implies that plastic deformation can occur by ideal shear without any dislocation activity. Indeed, the peculiar plastic deformation behaviors shown in Fig. 7, 9, and 10 are observed only in alloy compositions with the condition of e/a = 4.24 and Bo = 2.87. Further, work hardening hardly occurs at this alloy composition, which strongly suggests the possibility of a peculiar plastic deformation mechanism without the aid of any dislocation motion.

These considerations about the elastic constants and ideal shear strength explain well why both Young's modulus and WHR are minimized at the same specific condition. From these results, it is recognized that mechanical properties and plastic deformation behavior have strong correlations to β-phase stability in Ti-Nb-Ta-Zr-O alloys.

5. Conclusions

The authors investigated the effects of alloy content on mechanical properties and plastic deformation mechanisms to clarify the effect of β-phase stability on tensile properties and plastic deformation behavior in the Ti-Nb-Ta-Zr-O alloy system.

- The specific composition of e/a = 4.24 and Bo = 2.87 is the phase boundary between α″+β phases and β phase.
- Young's modulus and WHR are strongly correlated to β phase stability and indicate a minimum value at the alloy composition with e/a = 4.24 and Bo = 2.87.
- Plastic deformation behavior also correlates well with β-phase stability. Peculiar plastic deformation with giant faults in "Gum Metal" is observed at e/a = 4.24 and Bo = 2.87, but stress-induced martensitic transformation occurs in composition of e/a < 4.24 and Bo < 2.87 and dislocation glide occurs in composition of e/a > 4.24 and Bo > 2.87.
- The anisotropic elastic softening estimated by calculation signifies that ideal strength of the "Gum Metal" is a very small value that is close to the practical strength required for plastic deformation. This supports the possibility that the peculiar plastic deformation of "Gum Metal" was generated without the aid of dislocation glide.

References

1. T. Saito, T. Furuta, J.H. Hwang, S. Kuramoto, K. Nishino, N. Suzuki, R. Chen, A. Yamada, K. Ito, Y. Seno, T. Nonaka, H. Ikehata, N. Nagasako, C. Iwamoto, Y. Ikuhara, and T. Sakuma, Multifunctional Alloys Obtained via a Dislocation-Free Plastic Deformation Mechanism, *Science,* Vol 300, 2003, p 464-467
2. T. Furuta, K. Nishino, J.H. Hwang, A. Yamada, K. Ito, S. Osawa, S. Kuramoto, N. Suzuki, R. Chen, and T. Saito, Development of Multi Functional Titanium Alloy, "Gum Metal", *Ti-2003 Science and Technology; Proceedings of 10th World Conference on Titanium,* G. Lutjering and J. Albrecht, Ed., Jul 13-18, 2003 (Hamburg), Wiley, 2004, p 1519-1526
3. S. Kuramoto, T. Furuta, J.H. Hwang, Y. Seno, T. Nonaka, H. Ikehata,

N. Nagasako, K. Nishino, T. Saito, C. Iwamoto, Y. Ikuhara, and T. Sakuma, Origin for "Super" Properties in GUM METAL, *Ti-2003 Science and Technology; Proceedings of 10th World Conference on Titanium,* G. Lutjering and J. Albrecht, Ed., Jul 13-18, 2003 (Hamburg), Wiley, 2004, p 1527-1534
4. M. Morinaga, N. Yukawa, T. Maya, K. Sone, and H. Adachi, Theoretical Design of Titanium Alloys, *Sixth World Conference on Titanium,* P. Lacombe, R. Tricot, and G. Beranger, Ed., Jun 6-9, 1988 (Cannes), Les Editions de Physique, 1989, p 1601-1606
5. S. Hanada, T. Yoshio, and O. Izumi, Effect of Plastic Deformation Modes on Tensile Properties of Beta Titanium Alloys, *Trans. Jpn. Inst. Met.,* Vol 27, 1986, p 496-503
6. S. Hanada, M. Ozeki, and O. Izumi, Deformation Characteristics in β Phase Ti-Nb Alloys, *Metall. Trans. A,* Vol 16, 1985, p 789-795
7. H. Ikehata, N. Nagasako, T. Furuta, A. Fukumoto, K. Miwa, and T. Saito, First-Principles Calculations for Development of Low Elastic Modulus Ti Alloys, *Phys. Rev. B,* Vol 70, 2004, p 174113 (1-8)
8. C.R. Krenn, D. Roundy, J.W. Morris, Jr., and M.L. Cohen, Ideal Strength of bcc Metals, *Mater. Sci. Eng.,* Vol A319-321, 2001, p 111-114